OPEN ACCESS

Thermodynamic Evaluation of Five Organic Carbonates and Their Mixtures Used in Lithium Ion Batteries

View the article online for updates and enhancements.

You may also like

- Effects of Electrolyte Composition on Lithium Plating in Lithium-Ion Cells
  M. C. Smart and B. V. Ratnakumar

- The Effect of Additives upon the Performance of MCMB/LiNi$_x$Co$_{1-x}$O$_2$ Li-Ion Cells Containing Methyl Butyrate-Based Wide Operating Temperature Range Electrolytes
  Marshall C. Smart, Brett L. Lucht, Swapnil Dalavi et al.

- Effect of Lewis Acids on Graphite-Electrode Properties in EC-Based Electrolyte Solutions with Organophosphorus Compounds
  Shigetaka Tsubouchi, Shohei Suzuki, Katsunori Nishimura et al.

Thermodynamic Evaluation of Five Organic Carbonates and Their Mixtures Used in Lithium Ion Batteries

Peter Franke[z] (ORCID)

Karlsruhe Institute of Technology, Institute for Applied Materials – Applied Materials Physics (IAM-AWP), Karlsruhe, 76021, Germany

A thermodynamic database for 5 organic carbonates is compiled based on data from the literature. It includes the cyclic compounds ethylene carbonate (EC) and propylene carbonate (PC) as well as the linear carbonates dimethyl carbonate (DMC), diethyl carbonate (DEC), and ethyl methyl carbonate (EMC). For all of these substances the solid, liquid and gaseous phases are assessed. The solid phases are all treated as pure substances. In the liquid state, the cyclic compounds (EC+PC) form practically an ideal mixture which is also the case for the 3 binary combinations of the linear carbonates (DMC+DEC, DMC+EMC, DEC+EMC). The 6 binary liquids consisting of a linear and a cyclic carbonate exhibit all positive deviations from Raoult's law. The gas phase is described by an ideal mixture of the 5 substances for temperatures up to 1000 K and pressures slightly above normal pressure. The Gibbs energy functions of all compounds are related to the SGTE data of pure elements (here C, H, and O) by adjusting the standard quantities of formation ($\Delta_f H°$, $\Delta_f S°$) to experimental data.

Lithium-ion rechargeable batteries are widely used as power sources for many devices from portable electronics to electrical vehicles. Ideally, the electrolyte solution in these batteries is just a medium that allows the charge transport of Li-ions between the electrodes, but which itself is not involved in the electrochemical reactions. However, the solvents used here are frequently organic carbonates, the stability of which depends not only on the temperature but also on the oxidation and reduction potentials at the electrodes.

In Li-ion batteries, cyclic and linear organic carbonates are mixed to optimize the properties of the solvent. The cyclic carbonates have high dielectric constants (comparable to that of water), which increase the solubility of salts, but also relatively high viscosities, which lead to small diffusion coefficients and thus to low ionic conductivities. Linear organic carbonates have an inverse relationship between these two properties. The 5 most important technical carbonates used in Li-ion batteries are listed in Table I.

In thermodynamics, the stability of these solutions is described by the Gibbs energy functions of the pure substances, as well as their mixing behavior using appropriate interaction parameters. Thermodynamic datasets for calculating the mixing behavior and phase transformations of various organic carbonates have already been published in the literature, e.g.[1,2] However, in these evaluations so far the reference to the standard formation reactions from the elements is missing, which is necessary to calculate combustion reactions of carbonates or their decomposition at higher temperatures. Furthermore, the datasets[1,2] do not include a gas phase which is needed to model evaporation effects at the approach of a thermal runaway.

Thermodynamic Models

The Gibbs energy of a compound i in a liquid or solid phase ϕ is a function of the temperature only, $G_i^\phi(T)$, provided the pressure is kept at sufficently low levels[3]:

$$G_i^\phi = a + b\,T + c\,T \ln T + d\,T^2 + e\,T^3 + f\,T^{-1} + g\,T^7 + h\,T^{-9} \quad [1]$$

[z]E-mail: Peter.Franke@kit.edu

The entropy, enthalpy and heat capacity can be derived from the Gibbs energy:

$$S_i^\phi = -b - c - c \ln T - 2d\,T - 3e\,T^2 + f\,T^{-2}$$
$$-7g\,T^6 + 9h\,T^{-10} \quad [2a]$$

$$H_i^\phi = a - c\,T - d\,T^2 - 2e\,T^3 + 2f\,T^{-1} - 6g\,T^7 + 10h\,T^{-9} \quad [2b]$$

$$Cp_i^\phi = -c - 2d\,T - 6e\,T^2 - 2f\,T^{-2} - 42g\,T^6 - 90h\,T^{-10} \quad [2c]$$
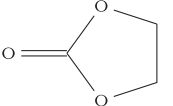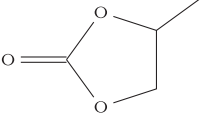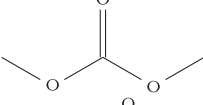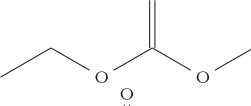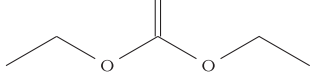
However, the temperature range of the thermodynamic functions usually has to be divided into several intervals, due to two reasons. Firstly, the temperature function cannot represent the thermodynamic property (G, S, H, C_P) sufficiently accurate over the given temperature range. The inclusion of additional terms with higher powers of T can improve the fit in the interval, but usually results in the function not being able to be extrapolated to higher or lower temperatures, since strong deviations occur just outside the range considered.

Secondly, when extrapolating the heat capacity of a liquid into the range of the supercooled melt or when extrapolating the functions of a solid into the superheated region, a situation can arise in which the solid has a higher entropy than the liquid at the same temperature, which contradicts common thermodynamic principles. The case when the entropy of a supercooled melt becomes smaller than the entropy of the crystalline solid is known in the literature as the Kauzmann paradox.[4] In real liquids, this situation is avoided by the transition into the glassy state. Unfortunately, for many liquids, no measurements of the enthalpy or heat capacity in the supercooled region or even in the glassy region are available. Therefore, in the course of thermodynamic modelling of the elements, SGTE proposed that the heat capacity of the supercooled liquid should approach the C_P function of the crystalline phase by adding an additional temperature interval below the melting temperature and using the T-term with the coefficient g (Eqs. 1, 2a-2c) to achieve the asymptotic transition.[5] Accordingly, the T-term with the coefficient h is used to make the heat capacity of the superheated solid approach that of the liquid.

For a gaseous compound, the Gibbs energy has a pressure-dependent contribution which is in the case of an ideal gas:

Table I. Organic carbonates assessed in the present investigation.

Compound	Abbreviation	Formula	Structure
Ethylene carbonate	EC	$C_3H_4O_3$	
Propylene carbonate	PC	$C_4H_6O_3$	
Dimethyl carbonate	DMC	$C_3H_6O_3$	
Ethyl methyl carbonate	EMC	$C_4H_8O_3$	
Diethyl carbonate	DEC	$C_5H_{10}O_3$	

$$G_i^{\text{gas}}(T, P) = G_i^{\text{gas}}(T) + RT \ln(P/P^\circ), \qquad [3]$$

where $P^\circ = 100 \text{kPa}$ is the reference pressure and R is the gas constant.

In the present work, the mixing thermodynamics of the carbonates is described by a simple model in which an ideal entropy of mixing is assumed and the enthalpy of mixing is represented by a Redlich-Kister polynomial of the mole fractions x_i. Thus, the Gibbs energy of a mixture consisting of n compounds is given by:

$$G_{\text{mix}}^{\phi} = \sum_{i=1}^{n} x_i G_i^{\phi} + RT \sum_{i=1}^{n} x_i \ln x_i$$
$$+ \sum_{i=1}^{n-1} \sum_{j>i}^{n} x_i x_j \sum_{k=0}^{m} {}^{k}L_{ij}(x_i - x_j)^k \qquad [4]$$

Here, G_i^{ϕ} denotes the Gibbs energy of the pure compound i in the phase ϕ, as given by Eq. 1. The coefficients of the Redlich-Kister polynomial, ${}^{k}L_{ij}$, are the mixing parameters of order k. In the present assessment their maximum order is m = 2. The constant n denotes the number of components in the mixture.

Assessment of the Pure Carbonates

For the thermodynamic description of the pure carbonates, their Gibbs energy functions have to be determined in the gas phase, in the liquid and in the solid modifications. For this purpose, the literature data for the heat capacities are used, as well as the temperatures and transformation enthalpies of the melting points and, if applicable, the corresponding data for polymorphic transformations in the solid state. The enthalpies of transformation into the gaseous state are derived from experimental vapor pressure curves.

The literature data for the entropies of the phases are based mainly on two methods. In the case of solid phases, the ratio C_P/T is integrated numerically, provided that the heat capacity has been determined over a temperature range which approaches sufficiently close to zero temperature.

In the case of gases, the entropies can be calculated from the corresponding partition functions, whose energy levels were determined spectroscopically using infrared and Raman investigations.

If the entropy is only known for the solid or gaseous state, the values in the other phases can be calculated from the data of the transformation points ($\Delta_{\text{tr}}S = \Delta_{\text{tr}}H/T_{\text{tr}}$) and the corresponding C_P functions.

The aim of a thermodynamic assessment is to determine the G-functions of all phases in the system. Thus, the coefficients (a to h) of Eq. 1 and the interaction parameters ${}^{k}L_{ij}$ of Eq. 4 have to be fitted to appropriate experimental data. This task is accomplished in the present work by using the PARROT module of the Thermo-Calc program.[6] Furthermore, all thermodynamic calculations and the diagrams in the present work are prepared with this program.

Ethylene carbonate.—In addition to the gas and the liquid phase, ethylene carbonate is known to occur also in a solid phase which belongs to the monolinic space group C2/c.[7]

The heat capacity of the condensed phases of EC is given in several experimental reports shown in Fig. 1a.[2,8–11] It can be seen that the values for the liquid of Vogdanis et al.[9] are significantly higher than those of the other investigations. Therefore, the values of this study were not taken into account when optimizing the heat capacity of liquid EC. The resulting best fit curves of the calculation represent the selected data in good agreement. In the Supplemental Information, the heat capacity of the condensed phases is shown with increased resolution, figure S1.

For the gas phase, results from two sources are available,[8,11] which are in good agreement with each other, as shown in Fig. 1a. The calculated best fit curve also represents the two data sets very well over the temperature range $100\text{K} < T < 1000\text{K}$. To achieve this agreement, it was necessary to split the function $G(T)$ into two temperature intervals. At the interval boundary at T=500 K, the two parts of the G function are calculated in such a way that the C_P function has the same slope on either side of the boundary.

In Fig. 1b, the calculated vapor pressure curve of EC is shown in comparison with the experimental data for the liquid[10–13] and the solid,[11,14] over a range of more than five orders of magnitude of pressure. Looking closely at the vapor pressure curve for the liquid, it is seen that the values in the van't Hoff plot do not lie on a straight line but on a slightly curved graph. The reason for this behavior is that the enthalpy of vaporization changes slightly with temperature, since the heat capacities of gas and liquid also change with temperature. In the literature, this behavior is often described by

(a)

(b)
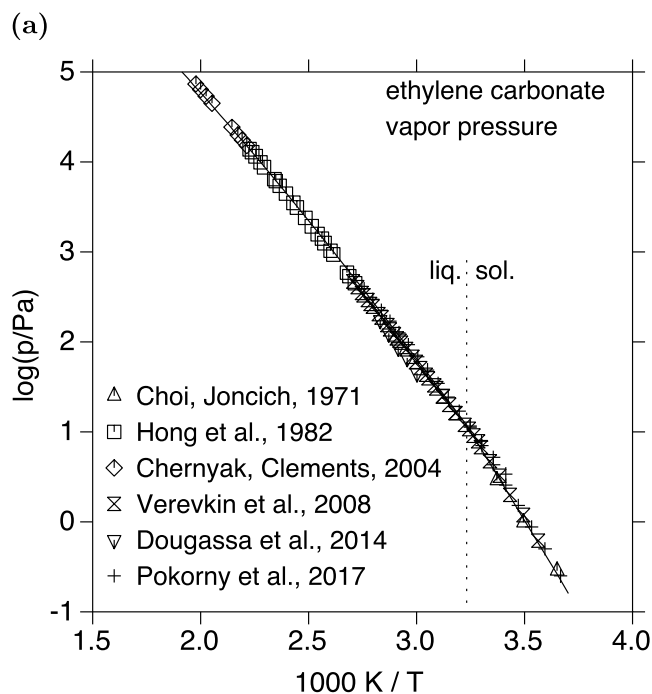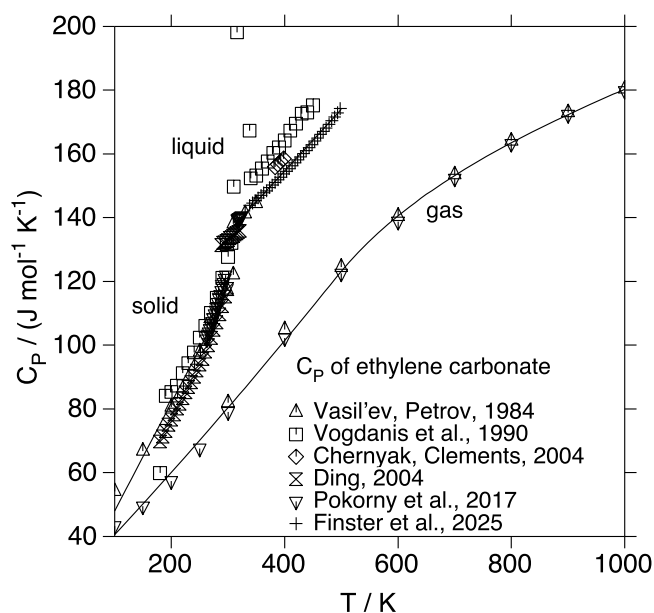
Figure 1. Thermochemical properties of ethylene carbonate: (a) heat capacity (see also supplementary figure S1), (b) vapor pressure.

phenomenological Antoine equations, whereas here it is a thermodynamically consistent result from the equilibrium calculations using the G-functions (Eq. 1) for the gas and the condensed phase.

At the intersection of the vapor pressure curves for the liquid and solid phases, a three-phase equilibrium exists in which the chemical potential of EC has the same value in all phases. Furthermore, the melting temperature and melting enthalpy of EC have been determined in several experimental investigations,[2,8,11,12,15] which are shown in Table II. In the thermodynamic optimization, the coefficients of the G functions of all phases (Eq. 1) are determined simultaneously so that the resulting data sets of the phases are consistent with each other. The calculated temperatures and transformation enthalpies of the phase equilibria are shown by bold face numbers in Table II.

No literature sources are given for the boiling point data in this table, since all these values are derived from the vapor pressure curves (at standard pressure, 101.325 kPa). The references to the respective experimental publications can be found in the vapor pressure diagrams instead. In addition to the enthalpies of vaporization at the corresponding boiling temperatures, the table also shows the calculated enthalpies of vaporization at 298.15 K. As discussed above, the two enthalpies differ due to the temperature-dependent heat capacities of the liquid and gaseous phases.

In order to calculate chemical reactions involving the carbonates considered here, it is necessary to know their enthalpies of formation and also their entropy values under standard conditions. The enthalpies of formation are usually determined by combustion calorimetry from the corresponding enthalpies of combustion. The entropy values for condensed phases are calculated from their heat capacities, provided that these are known down to sufficiently low temperatures. In the case of gases, their entropy values can be calculated using partition functions based on spectroscopically determined transition energies.

The entropy of the carbonates in their various states of aggregation are listed in Table III as well as their enthalpies of formation under standard conditions. The bold face numbers are the respective values calculated with the dataset of the present work. For EC, entropy values are reported by two investigations[8,11] in good agreement for the gas phase. The standard enthalpy of formation of EC is reported several times.[9,16–19] Here it is noticeable that the value given by Choi and Joncich[16] is significantly more negative than in the other four studies. This discrepancy is also repeated for the other carbonates. Therefore, the enthalpies of formation reported by Choi and Joncich[16] have been omitted from the optimisation of the thermodynamic functions of EC and the other carbonates.

Propylene carbonate.—In propylene carbonate, the carbon atom on which the methyl group is located is an optically active center, resulting in two different molecules which are mirror images of each other. Which of these enantiomers are formed in a synthesis and in what ratio depends on the production routes used. In Li-ion batteries, only racemic mixtures are used, which contain the enantiomers in an equimolar ratio. Accordingly, racemic mixtures are used in all of the studies of propylene carbonate considered here. Since the mixing ratio in the racemate does not change during phase transformations, propylene carbonate is formally treated as a pure substance when modeling the phases.

Propylene carbonate is known to exist in several states, the gaseous, liquid, crystalline and two glassy states.[20]

The heat capacity of the condensed phases of PC is given in several experimental reports shown in Fig. 2a.[2,8,10,11,20–22] It can be seen that the values for the liquid of Comelli et al.[22] are noticeably higher and those of Ding[2] are significantly lower than those of the other five investigations. Therefore, the values of these two studies were not taken into account when optimizing the heat capacity of liquid PC. Heat capacities in the glass range have been reported solely by Fujimori and Oguni.[20] According to their results, the glass transition temperature is at $T_g = 156$K and additionally, a second transformation within the glass range was detected at 64 K based on a very small jump in the data of the heat capacity. However, due to the smallness of this jump the transition between the two glass states is neglected in the present assessment. Furthermore, the temperature function for the glass is attached to that of the liquid using an additional temperature range below T_g.

After appending the G-function of the glass state to that of the supercooled liquid the Kauzmann paradox does not occour in the dataset of PC, which was verified by calculating the entropy of the phases over the temperature range up to 1000 K. Therefore, it was not necessary to introduce additional temperature intervals into this dataset.

The heat capacity of gaseous PC is reported by the same two sources as in the case of EC,[8,11] and as before, their results are in good agreement as shown in Fig. 2a. In order to achieve the good fit

Table II. Phase transition data for the carbonates.

Compound	Transition Reference	T (K)	$\Delta_{tr}H$ (kJ mol^{-1})
EC	sol./liq.	**309.4**	**13.3**
	2	311.2	13.02
	8	309.49	13.3
	11	309.13	13.5
	12	309.2	13.3
	15	309.52	13.19
	liq./gas	**523.3**	**50.5**
		298.15	**62.4**
PC	sol./liq.	**218.6**	**8.0**
	2	220.3	8.96
	8	224.85	9.62
	20	218.66	8.011
	liq./gas	**515.8**	**48.3**
		298.15	**61.1**
DMC	sol./liq.	**277.9**	**11.7**
	2	278.2	11.58
	28	277.57	11.9
	liq./gas	**362.8**	**34.5**
		298.15	**38.4**
DEC	sol./liq.	**198.2**	**9.2**
	2	198.2	9.24
	28	196.4	9.1
	liq./gas	**399.5**	**37.6**
		298.15	**44.5**
EMC	sol./liq.	**219.4**	**11.2**
	2	219.4	11.24
	12	219.7	11.5
	liq./gas	**381.3**	**36.1**
		298.15	**40.7**

Note. The entries in bold face denote results of this work. Numbers in column 2 are references.

Table III. Entropy and standard enthalpy of formation for the carbonates at 298.15 K.

Compound	Phase	S_{298} (J mol^{-1} K^{-1})		$\Delta_f H°_{298}$ (kJ mol^{-1})	
EC	solid	**129.3**		**−585.9**	
		132.5	8	−590.9	9
				−682.8	16
				−584.8	17
				−581.6	18
				−586.3	19
	liquid	**171.7**		**−572.7**	
	gas	**298.0**		**−510.4**	
		294.4	8	−604.3	16
		301.6	11	−510.7	17
PC	solid	**160.3**		**−625.1**	
	liquid	**210.3**		**−613.7**	
		218.6	8	−631.8	16
		212.5	20	−614.1	17
				−613.4	18
	gas	**336.4**		**−552.6**	
		337.9	11	−601.2	16
				−553.9	17
DMC	solid	**188.9**		**−621.2**	
	liquid	**232.5**		-609.1	
				−608.7	37
	gas	**339.6**		**−570.7**	
		339.6	28	−571.0	37
DEC	solid	**252.2**		**−692.3**	
	liquid	**303.0**		**−682.1**	
				−727.2	16
				−681.5	46
	gas	**417.2**		**−637.6**	
		417.2	28	−684.2	16
				−637.9	46
EMC	solid	**217.9**		**−656.5**	
	liquid	**269.6**		**−645.2**	
	gas	**378.0**		**−604.5**	

Note. The entries in bold face denote results of this work. Numbers in columns 4 and 6 are references.

of the calculated C_P function to the experimental data for PC, the temperature range was again divided at T=500 K into two intervals, under the condition that the C_P function has the same slope on both sides of the joint.

In Fig. 2b, the calculated vapor pressure curve of liquid PC is shown in comparison with experimental data over a range of five orders of magnitude of the pressure.[10,11,13,14,16,23–25] It can be seen that the experimental data are generally in good agreement among each other and that they are well represented by the calculated curve. Only two experimental points from the set of Choi and Joncich[16] are noticeably above the fitted curve and two points from the set of Nasirzadeh et al.[24] are below the curve. These points were excluded from the thermodynamic optimization. Besides these investigations, Wilson et al.[26] have reported measurements of the boiling temperature under elevated pressures in the range of 13–40 bar. However, under these conditions the gaseous PC shows noticeable deviations from the ideal gas behavior and therefore, the corresponding results of Wilson et al. have not been included in the present evaluation.

The calculated phase transition data for PC are shown in Table II and compared with experimental values.[2,8,20] Liquid PC can be supercooled very easily, which makes the determination of the melting point difficult. In the calorimetric investigations by Fujimori and Oguni,[20] the thermodynamic properties of PC were determined both in its stable states and in the supercooled liquid and glassy states. Therefore, when optimizing the dataset for PC, the results of Fujimori and Oguni were given a high weight. The theoretical background of applying weight factors in optimization programs based on the minimization of square sums is explained in chapter 2 of the book by Lukas et al.[3] The details of how these weightings are applied in the PARROT module are described in the user manual of

the Thermo-Calc program,[6] which is available online (http://thermo-calc.com).

The calculated entropy values for PC and its standard enthalpy of formation at room temperature are compared with experimental values in Table III. As previously for EC, the higher value of Choi and Joncich[16] was not taken into account in the data optimization.

***Dimethyl carbonate.*—**Dimethyl carbonate can occur in the gaseous, liquid, and in three crystalline orthorhombic phases.[27] In the sequence from high to low temperatures these solids belong to the space groups Ibam, Pbcm, and Pbca. At present, no thermodynamic data seem to be known for the crystals with the space group Pbca and therefore, this phase is omitted from the present evaluation. The high temperature solid is denoted here as DMCH and the crystalline phase with the space group Pbcm is denoted as DMCL. The heat capacity of these two phases has been measured by Ding[2] and for part of the DMCH phase also by Pokorný et al.[28] The phase transformation between DMCH and DMCL occours at 220.1 K and according to the shape of the C_P curve it is of 2nd order.[2] This result was confirmed by the crystallographic investigation of Whitfield,[27] who found an order/disorder relation between the crystal structures of DMC in the Pbcm and Ibam space groups.

In the dataset the course of the C_P function is described by splitting the temperature range at 220.1 K into two intervals with

(a)

(b)
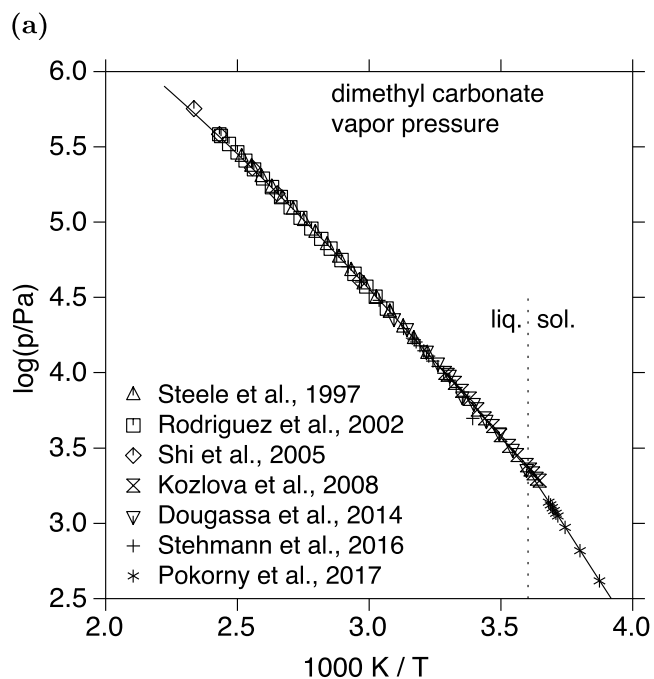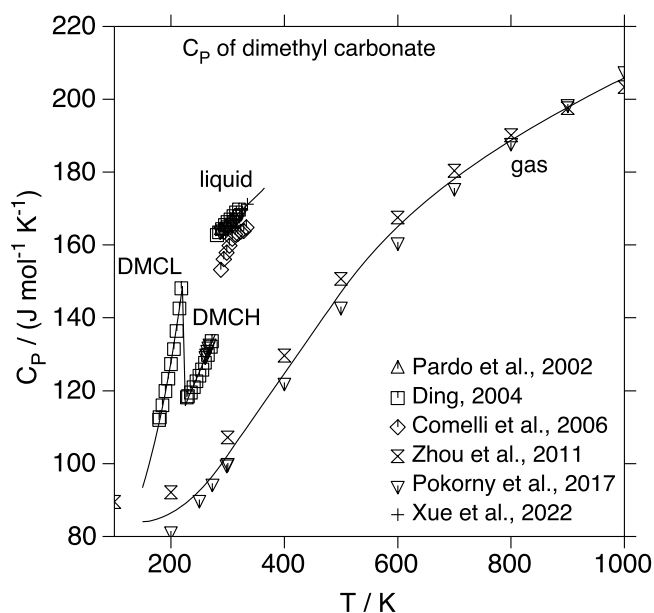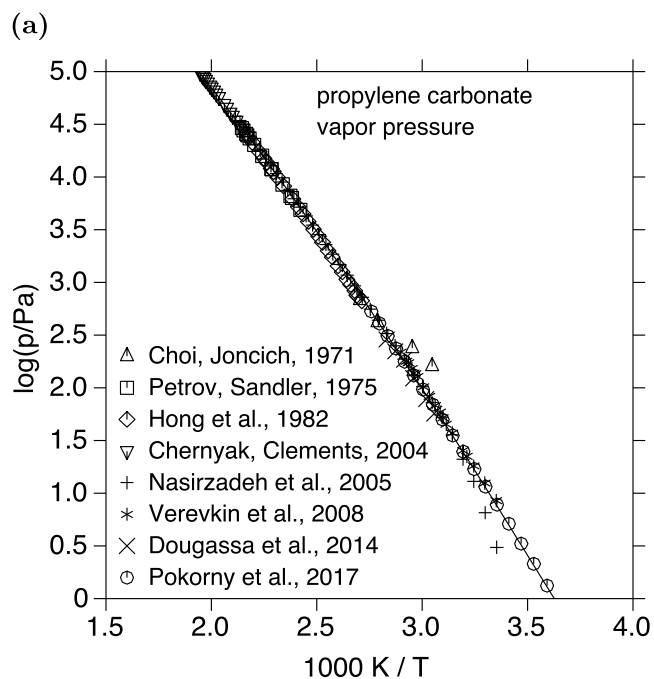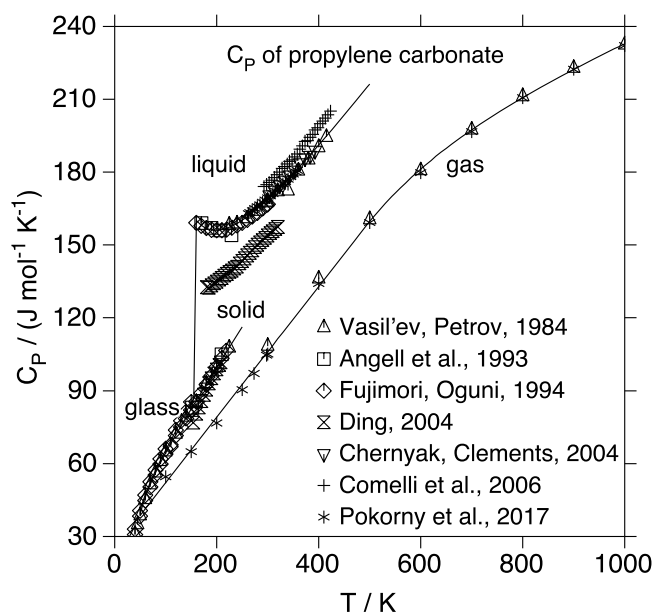
Figure 2. Thermochemical properties of propylene carbonate: (a) heat capacity (see also supplementary figure S2), (b) vapor pressure.

(a)

(b)

Figure 3. Thermochemical properties of dimethyl carbonate: (a) heat capacity (see also supplementary figure S3), (b) vapor pressure.

appropriate temperature functions according to Eq. 2c as can be seen in Fig. 3a.

The heat capacity of liquid DMC has been measured in five investigations and the results of four reports are in close agreement with each other.[2,28–30] Only the values measured by Comelli et al.[22] are significantly lower and they have been omitted from the optimisation. Figure 3a shows that the C_P values of the liquid are well represented by a linear function.

The heat capacity of gaseous DMC has been reported by Pokorný et al.[28] and by Zhou et al.[31] Here, it should be noted that Zhou et al.[31] do not provide a table of C_P values, but instead a formula for C_P derived from the equation of state. The corresponding data shown in Fig. 3a are calculated using the equation of Zhou et al.[31] It can be seen that the C_P values of Zhou et al. are higher than those of

Pokorný et al., whereas the difference decreases at higher temperatures. The calculated curve represents an average of both datasets.

In Fig. 3b, the calculated vapor pressure curves for liquid DMC and solid DMCH are shown in comparison with experimental data.[25,28,32–36]

The melting point of DMC and its melting enthalpy are reported in good agreement by Ding[2] and Pokorný et al.,[28] as shown in Table II. The entropy of gaseous DMC at 298.15 K has been reported by Pokorný et al.[28] and the entropy values of liquid and solid DMC shown in Table III are calculated in the present work based on the data for the heat capacities and phase transition data. In addition, Table III lists the standard enthalpy of formation of liquid and gaseous DMC which has been determined by Steele et al.[37] based on combustion experiments.
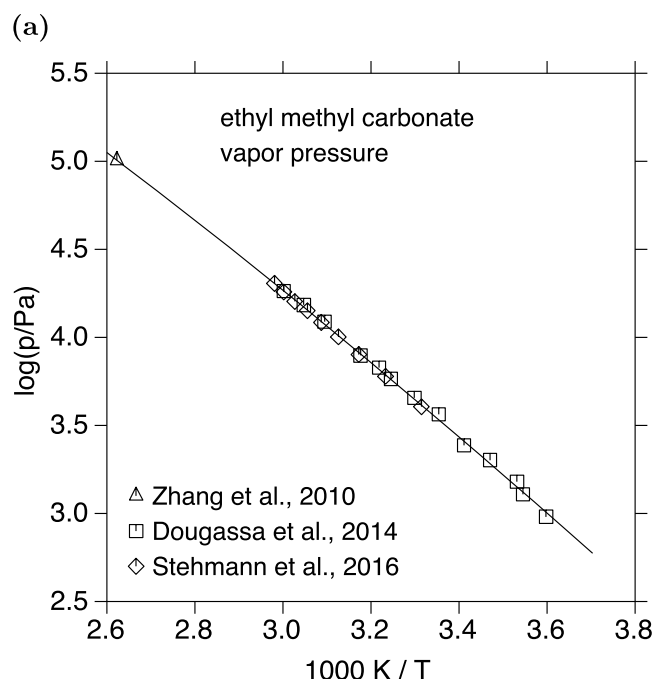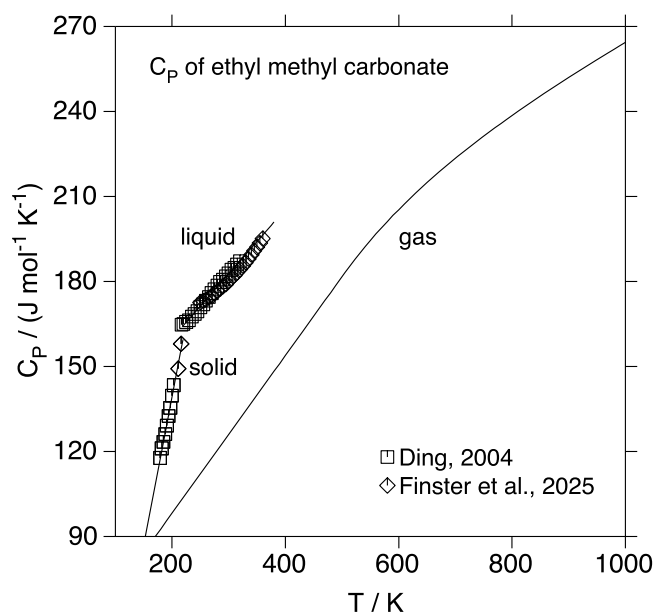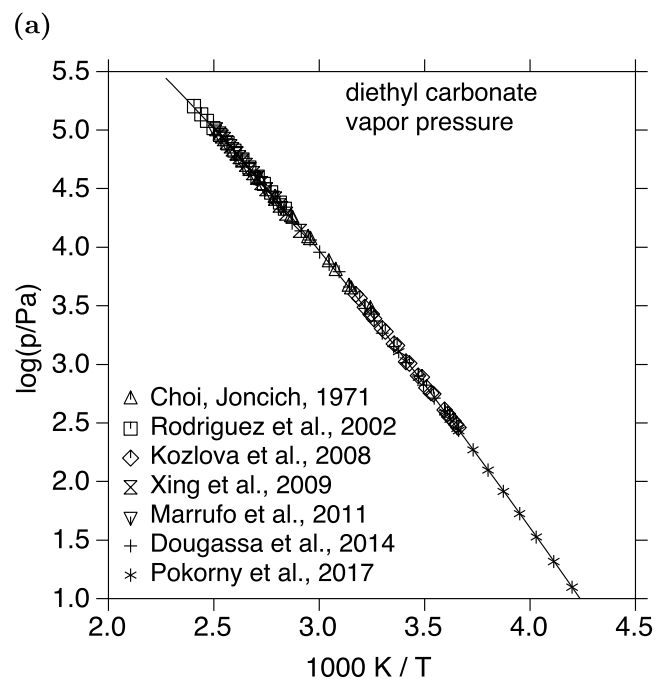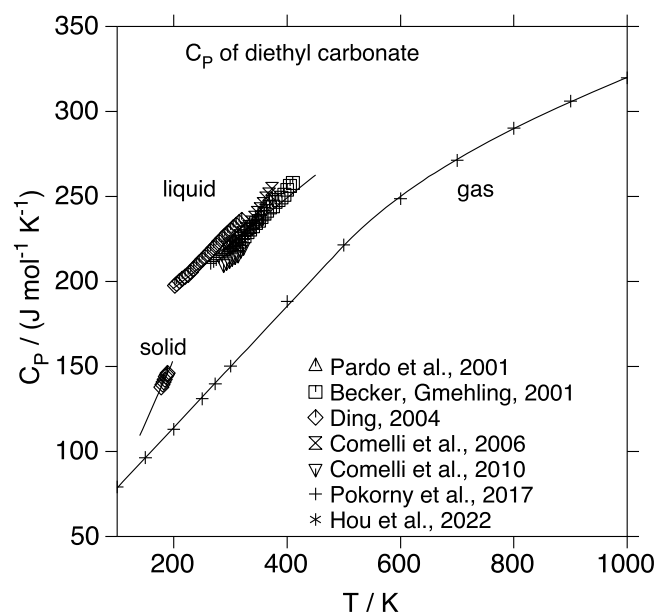
Figure 4. Thermochemical properties of diethyl carbonate: (a) heat capacity (see also supplementary figure S4), (b) vapor pressure.

Figure 5. Thermochemical properties of ethyl methyl carbonate: (a) heat capacity (see also supplementary figure S5), (b) vapor pressure.

Diethyl carbonate.—In addition to the gas and the liquid, diethyl carbonate can also occur in a crystalline state. According to Yakovenko et al. these crystals belong to the orthorhombic space group $Pna2_1$.[38]

Up to now, the heat capacity of the solid has been measured only by Ding,[2] and that of the gas has been reported only by Pokorný et al.[28] The liquid heat capacities of DEC have been reported by several investigations.[2,22,28,39–42] In Fig. 4a the calculated C_P functions for the three phases are compared with the experimental data. The experimental data for the liquid phase show noticeable differences between the different reports. However, they were all taken into account in the fit of a linear C_P function for the liquid. Figure 4b shows the the calculated vapor pressure curve for liquid DEC compared to the experimental data.[16,25,28,35,43–45]

The melting enthalpy and melting temperature have been reported in good agreement by Ding[2] and Pokorný et al.[28] In Table II these data are compared with the calculated values. The standard entropy of gaseous DEC has been determined by Pokorný et al.[28] and the corresponding values for the other phases of DEC shown in Table III have been calculated in the present work based on the assessed heat capacities and phase transition data. The standard enthalpy of formation of liquid and gaseous DEC have been reported by Choi and Joncich[16] and by Månsson.[46] As in the case of EC and PC before, the higher values of Choi and Joncich[16] were not considered in the present optimization.

Ethyl methyl carbonate.—The known phases of ethyl methyl carbonate are the gas, liquid and one crystalline solid. The heat

Table IV. Thermodynamic parameters of the carbonates.

Phase T-range (K)	Parameter (J mol^{-1})
Gas	
[100, 500)	$G_{\mathrm{DEC}}^{\mathrm{gas}} = -666230.8 - 23.552\,T - 42.9138\,T\ln T - 0.178147\,T^2 + RTLNP$
[500, 1000)	$-756382.6 + 1201.87\,T - 225.799\,T\ln T - 0.0545015\,T^2 + 7405060\,T^{-1}$ $+ RTLNP$
[100, 300)	$G_{\mathrm{DMC}}^{\mathrm{gas}} = -597385 + 293.597\,T - 99.0241\,T\ln T + 0.105595\,T^2 - 1.23519\cdot10^{-4}\,T^3$ $+ RTLNP$
[300, 500)	$-591170 - 36.1988\,T - 35.3564\,T\ln T - 0.111686\,T^2 + RTLNP$
[500, 1000)	$-651898 + 787.396\,T - 158.224\,T\ln T - 0.028834\,T^2 + 5001957\,T^{-1}$ $+ RTLNP$
[100, 500)	$G_{\mathrm{EC}}^{\mathrm{gas}} = -525406 - 95.7693\,T - 21.7384\,T\ln T - 0.0922116\,T^2 - 6.18674\cdot10^{-6}\,T^3$ $+ RTLNP$
[500, 1000)	$-582471 + 656.018\,T - 132.781\,T\ln T - 0.0284898\,T^2 + 4755090\,T^{-1}$ $+ RTLNP$
[100, 500)	$G_{\mathrm{EMC}}^{\mathrm{gas}} = -629563 - 9.76564\,T - 42.598\,T\ln T - 0.13907\,T^2 + RTLNP$
[500, 1000)	$-698178 + 908.917\,T - 179.345\,T\ln T - 0.048227\,T^2 + 5738000\,T^{-1}$ $+ RTLNP$
[50, 500)	$G_{\mathrm{PC}}^{\mathrm{gas}} = -572040 - 86.8996\,T - 25.281\,T\ln T - 0.13446\,T^2 + RTLNP$
[500, 1000)	$-639927.8 + 842.061\,T - 164.08\,T\ln T - 0.039911\,T^2 + 5531300\,T^{-1}$ $+ RTLNP$
Liquid	
[150, 198.2)	$G_{\mathrm{DEC}}^{\mathrm{liq}} = -719767.71 - 34.984682\,T - 4.35\,T\ln T - 0.375\,T^2 - 1.6700686\cdot10^{-14}\,T^7$
[198.2, 1000)	$-736498 + 732.75\,T - 142.8\,T\ln T - 0.133\,T^2$
[100, 277.9)	$G_{\mathrm{DMC}}^{\mathrm{liq}} = -636905.548 + 104.520189\,T - 32.97\,T\ln T - 0.1844\,T^2$ $- 1.3944696\cdot10^{-15}\,T^7$
[277.9, 1000)	$-651730 + 618.936\,T - 120.39\,T\ln T - 0.07565\,T^2$
[100, 309.42)	$G_{\mathrm{EC}}^{\mathrm{liq}} = -592638.22 + 25.757331\,T - 13.99\,T\ln T - 0.1699\,T^2 - 4.89631\cdot10^{-16}\,T^7$
[309.42, 1000)	$-604452 + 404.778\,T - 77.46\,T\ln T - 0.0965\,T^2$
[50, 219.4)	$G_{\mathrm{EMC}}^{\mathrm{liq}} = -668791.42 - 435.03662\,T + 70.27\,T\ln T - 0.5238\,T^2$ $- 1.0113047\cdot10^{-15}\,T^7$
[219.4, 1000)	$-689399 + 563.37\,T - 114.2\,T\ln T - 0.1142\,T^2$
[50, 156)	$G_{\mathrm{PC}}^{\mathrm{liq}} = -645760.48 + 136.45722\,T - 30.7\,T\ln T - 0.184\,T^2 + 10000\,T^{-1}$
[156, 1000)	$-644383 + 361.587\,T - 74.0\,T\ln T - 0.138\,T^2 - 537000\,T^{-1}$
[100, 1000)	${}^0L_{\mathrm{DMC,EC}}^{\mathrm{liq}} = 1650$, ${}^1L_{\mathrm{DMC,EC}}^{\mathrm{liq}}=250$, ${}^2L_{\mathrm{DMC,EC}}^{\mathrm{liq}}=200$
[100, 1000)	${}^0L_{\mathrm{EC,EMC}}^{\mathrm{liq}} = 2600$, ${}^1L_{\mathrm{EC,EMC}}^{\mathrm{liq}}=-320$, ${}^2L_{\mathrm{EC,EMC}}^{\mathrm{liq}}=-380$
[100, 1000)	${}^0L_{\mathrm{DEC,EC}}^{\mathrm{liq}} = 3760$, ${}^1L_{\mathrm{DEC,EC}}^{\mathrm{liq}}=500$, ${}^2L_{\mathrm{DEC,EC}}^{\mathrm{liq}}=700$
[100, 1000)	${}^0L_{\mathrm{DMC,PC}}^{\mathrm{liq}} = 890$, ${}^1L_{\mathrm{DMC,PC}}^{\mathrm{liq}}=460$
[100, 1000)	${}^0L_{\mathrm{EMC,PC}}^{\mathrm{liq}} = 1480$, ${}^1L_{\mathrm{EMC,PC}}^{\mathrm{liq}}=580$, ${}^2L_{\mathrm{EMC,PC}}^{\mathrm{liq}}=730$
[100, 1000)	${}^0L_{\mathrm{DEC,PC}}^{\mathrm{liq}} = 1760$, ${}^1L_{\mathrm{DEC,PC}}^{\mathrm{liq}}=290$, ${}^2L_{\mathrm{DEC,PC}}^{\mathrm{liq}}=680$
[100, 1000)	${}^0L_{\mathrm{EC,PC}}^{\mathrm{liq}} = 0$
[100, 1000)	${}^0L_{\mathrm{DMC,EMC}}^{\mathrm{liq}} = 0$
[100, 1000)	${}^0L_{\mathrm{DEC,DMC}}^{\mathrm{liq}} = 0$
[100, 1000)	${}^0L_{\mathrm{DEC,EMC}}^{\mathrm{liq}} = 0$
Solid phases	
[100, 309.42)	$G_{\mathrm{EC}}^{\mathrm{ECS}} = -605140 + 65.7316\,T - 13.99\,T\ln T - 0.1699\,T^2$
[309.42, 500)	$-618371.98 + 449.56484\,T - 77.46\,T\ln T - 0.0965\,T^2$ $+ 1.6130569\cdot10^{24}\,T^{-9}$
[100, 500)	$G_{\mathrm{PC}}^{\mathrm{PCS}} = -650017 + 167.205\,T - 34.18\,T\ln T - 0.165\,T^2 + 14000\,T^{-1}$
[100, 220.1)	$G_{\mathrm{DMC}}^{\mathrm{DMCH}} = -648836.55 + 149.14925\,T - 32.97\,T\ln T - 0.1844\,T^2 - 2.220\cdot10^{-12}\,T^6$
[220.1, 277.9)	$-647574.6 + 142.269\,T - 32.97\,T\ln T - 0.1844\,T^2$
[277.9, 500)	$-664303.011 + 663.878611\,T - 120.39\,T\ln T - 0.07565\,T^2$ $+ 8.2344119\cdot10^{23}\,T^{-9}$
[100, 220.1)	$G_{\mathrm{DMC}}^{\mathrm{DMCL}} = -648856.55 + 149.24012\,T - 32.97\,T\ln T - 0.1844\,T^2 - 2.220\cdot10^{-12}\,T^6$

Table IV. (Continued).

Phase T-range (K)	Parameter (J mol^{-1})
[220.1, 277.9)	$-647594.6 + 142.35987\,T - 32.97\,T\ln T - 0.1844\,T^2$
[277.9, 500)	$-664323.011 + 663.969481\,T - 120.39\,T\ln T - 0.07565\,T^2$
	$+ 8.2344119{\cdot}10^{23}\,T^{-9}$
[100, 198.2)	$G_{\text{DEC}}^{\text{DECS}} = -727804 + 4.54894\,T - 4.35\,T\ln T - 0.375\,T^2$
[198.2, 500)	$-746674.66 + 783.62261\,T - 142.8\,T\ln T - 0.133\,T^2$
	$+ 4.4197683{\cdot}10^{22}\,T^{-9}$
[50, 219.4)	$G_{\text{EMC}}^{\text{EMCS}} = -679882 - 384.60\,T + 70.27\,T\ln T - 0.5238\,T^2$
[219.4, 500)	$-700753.56 + 615.06996\,T - 114.2\,T\ln T - 0.1142\,T^2$
	$+ 1.3604256{\cdot}10^{22}\,T^{-9}$
Functions	
	$\text{RTLNP} = R T \ln(P/P^{\circ}), \qquad P^{\circ}=100\ \text{kPa}$

capacity has been determined for the solid and the liquid phase by Ding[2] and Finster et al.[12] The heat capacity in each phase can be described by a linear temperature function, as shown in Fig. 5a. Since no data are known for the heat capacity of the gas phase, this property is approximated by the average of the C_P data of DMC and DEC which are reported by Pokorný et al.[28] The resulting calculated function is shown in Fig. 5a with the label gas.

In Fig. 5b the calculated vapor pressure curve for liquid EMC is compared to the experimental data.[25,36,47] The melting enthalpy of EMC was first measured by Ding[2] and recently confirmed by Finster et al.,[12] as shown in Table II. No experimental results are known so far for the standard enthalpy of formation as well as the entropy of EMC at room temperature. Therefore, in the present assessment we assume that the entropy of gaseous EMC is the average of the corresponding values of DMC and DEC. The same assumption holds for the standard enthalpy of formation of EMC, resulting in the values shown in Table III.

Assessment of the Binary Systems

The combination of the five pure carbonates results in ten binary systems. The phase diagrams of all these systems were investigated in the range of solid/liquid equilibria by Ding using calorimetric methods.[2] Furthermore, Ding also investigated the boiling curves in the two systems PC–EC and PC–DEC.[48] In addition, for PC–DEC the results of Hu et al. are available.[49] In other systems the gas/liquid equilibria have been investigated by different authors. Luo et al.[50] determined the boiling and dew curves in the phase diagrams of DEC–DMC and PC–DMC, and Zhang et al.[47] determined them in the systems DEC–EMC and EMC–DMC. In the DMC–EC system, the evaporation equilibria were determined by Fang et al.,[51] and in the DEC–EC system by Nagl et al.[52]

In the thermodynamic evaluation of the binary systems, some simplifying assumptions are made. The crystalline phases of the carbonates are treated as pure phases. This assumption is supported by the fact that no solubility ranges in the solids have been discovered in the experiments so far. The gas phase is treated as an ideal gas, and the justification of this approach has to be veryfied afterwards by comparing the calculations with the experimental data. The liquid is modeled as a generalized regular solution, as shown in Eq. 4. The PARROT module of the Thermo-Calc program[6] is used again to determine the mixing parameters in the liquid ($^{k}L_{ij}$). The mixing parameters are varied so that the calculated phase diagram achieves the closest fit to the experimental data. By this procedure a temperature range is covered from the sub-solidus domain up to the gas phase at normal pressure (101.3 kPa). The optimized parameters of the pure compounds as well as the interaction parameters $^{k}L_{ij}$ are listed in Table IV. When modeling the thermodynamic functions, it is often necessary to divide the equations into two or more

temperature intervals, as discussed previously. In Table IV an interval between the temperatures T_1 and T_2 is represented by the notation [T_1, T_2) which means $T_1 \leqslant T < T_2$. For calculations with the Thermo-Calc software, the thermodynamic parameters of Table IV are transferred to the programs via a specially formatted file (TDB). A corresponding listing of this thermodynamic database is provided in the Supplementary Information.

According to the mixing behavior in the liquid, the systems can be divided into two groups. In systems with ideal mixing in the liquid all mixing parameters are zero, which is the case when both components are either cyclic (PC–EC) or both components are linear (DEC–DMC, DEC–EMC, and EMC–DMC). The other group contains the systems with one cyclic and one linear component. These systems show positive deviations from Raoult's law and the mixing enthalpies are endothermal.
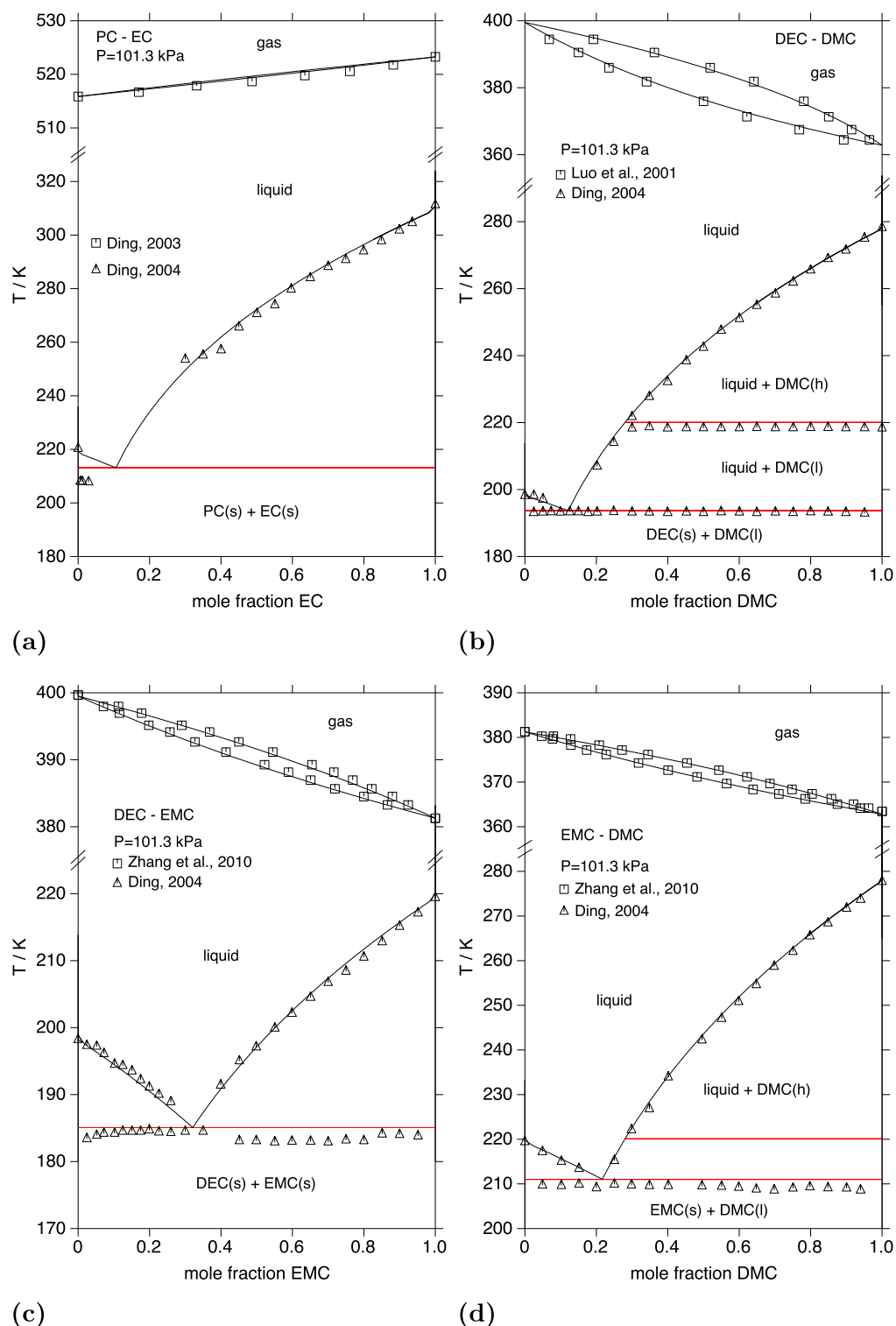
The phase diagrams of the four systems with ideal mixing in the liquid phase are shown in Fig. 6. It can be seen that the calculations are generally in good agreement with the experimental data except for a small deviation in the system PC–EC (Fig. 6a). Here, the eutectic temperature is calculated to be 213.1 K, while the experimental value is 207.9 K.[2] It is possible to achieve a notably better value for the eutectic temperature using a higher order Redlich-Kister polynomial. However, in this case the corresponding excess parameters of the liquid lead to significant deviations of the boiling curve from the experimental values. Therefore, the ideal mixing behavior for the liquid in the PC-EC system is retained in the present data set.

The phase diagrams of the non-ideal systems of ethylene carbonate combined with the three linear carbonates are shown in Fig. 7. It can be seen that all calculated phase equilibria are well supported by the experimental results. Only in the case of EMC-EC (Fig. 7c) no experimental data are available for the boiling range.

The three phase diagrams of PC mixed with linear carbonates are shown in Fig. 8. As before, no data for boiling equilibria are available for the system involving EMC (Fig. 8c). The successful calculation of all 10 phase diagrams confirms the simplifying assumptions in the thermodynamic modeling of the phases presented above.

Discussion

The assessed functions for the Gibbs energies of the organic carbonates given in Table IV are compatible with the SGTE Substance Database which contains thermodynamic data of pure substances, including for example H_2O, CO_2, CH_4, and many more. By combining the dataset for the carbonates and the SGTE database, chemical reactions with participation of the carbonates can be calculated. Among them, the decomposition reactions are of special interest which are shown in Table V. It can be seen that all these

Figure 6. Phase diagrams of binary carbonate systems with ideal mixing in the liquid: (a) PC–EC, (b) DEC–DMC, (c) DEC–EMC, (d) EMC–DMC.

reactions have a quite strong negative $\Delta_r G$, which means that the thermodynamic equilibria are strongly shifted to the side of the decomposition products. Therefore, all these carbonates are only metastable, similar to many other organic substances. Of course, the carbonates can be produced and stored at room temperature for considerable periods of time, but nevertheless they will decompose if enough activation energy is provided or if suitable catalysts are present.

Besides the equations shown in Table V many other reactions are conceivable, but those given here lead to the most stable sets of products. Although the carbonates have high thermodynamic driving forces for decay, they are still durable enough to allow experimental investigations of phase equilibria up to their boiling temperatures.

The thermodynamic data of the carbonates from the present evaluation can be compared with the respective results reported by Liu[1] and Shurtz and Hewson.[53] Thermodynamic data of three
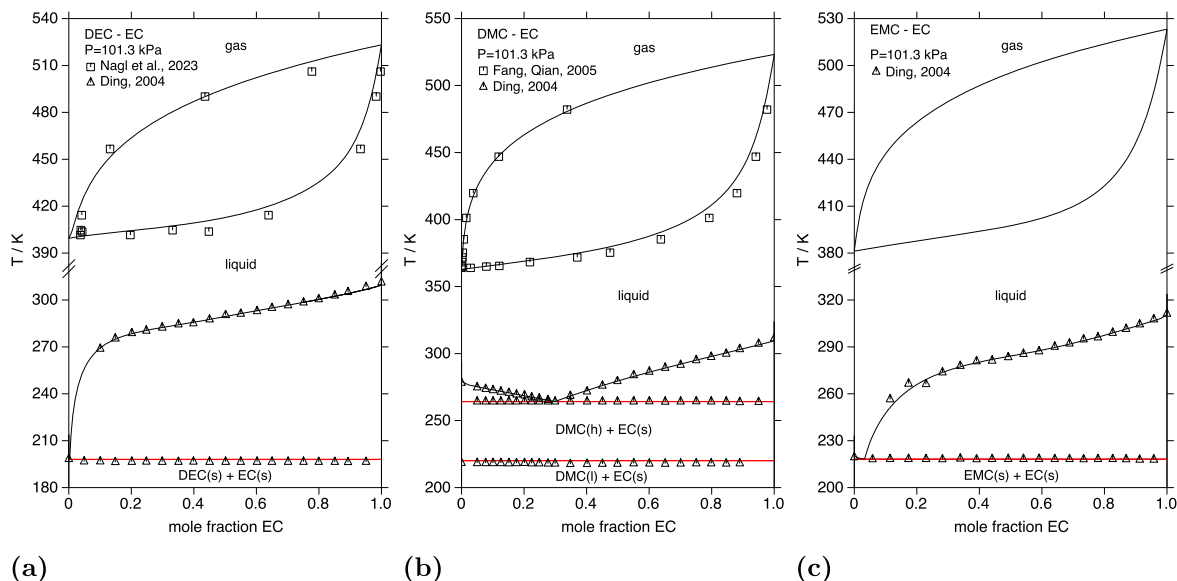
Figure 7. Phase diagrams of ethylene carbonate with linear carbonates: (a) DEC–EC, (b) DMC–EC, (c) EMC–EC.
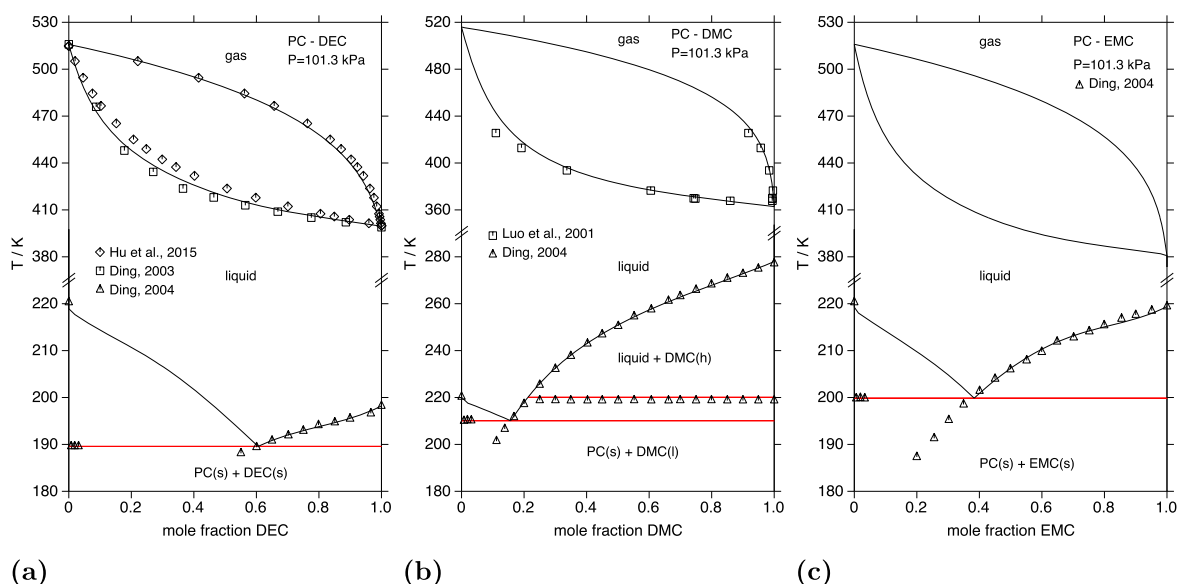

Figure 8. Phase diagrams of propylene carbonate with linear carbonates: (a) PC–DEC, (b) PC–DMC, (c) PC–EMC.

Table V. Decomposition of the carbonates into the most stable products at 298.15 K.

Carbonate	Decomposition reaction at 298.15 K	$\Delta_r G$ (kJ mol^{-1})	$\Delta_r H$ (kJ mol^{-1})
EC	$C_3H_4O_3(s) \rightarrow 2H_2O(l) + 21/2C(s) + 1/2CO_2(g)$	−221.9	−181.8
PC	$C_4H_6O_3(l) \rightarrow 3H_2O(l) + 4C(s)$	−250.5	−243.8
DMC	$C_3H_6O_3(l) \rightarrow 3H_2O(l) + 3C(s)$	−246.8	−248.4
EMC	$C_4H_8O_3(l) \rightarrow 3H_2O(l) + 31/2C(s) + 1/2CH_4(g)$	−265.6	−248.9
DEC	$C_5H_{10}O_3(l) \rightarrow 3H_2O(l) + 4C(s) + CH_4(g)$	−284.7	−248.6

carbonates (DMC, EC, and PC) are presented in Table II of Liu's assessment.[1] Here, only the quantities $\Delta_f H°_{298}$ for EC and S_{298} for EC and PC are in reasonable agreement with the corresponding values in Table III of the present work. But $\Delta_f H°_{298}$ for PC and DMC and S_{298} for DMC differ drastically from the data of present work. The data for the melting equilibria reported by Liu[1]

are mostly in fair agreement with the values in Table II of the present work, except for the melting point of PC, which is noticeably lower in the present work (218.6 K) due to a high weight given to the investigation of Fujimori and Oguni.[20]

In the review of Shurtz and Hewson[53] (Table VII) several thermodynamic data for the five carbonates (EC, PC, DMC, EMC,

DEC) are compiled from the literature. In comparison with the values for $\Delta_f H°_{298}$ listed in Table III of the present work, there is generally good agreement, but most entropy values show significant deviations. However, in an erratum which has been published during the review process of the present manuscript, Shurtz and Hewson[54] provide values in close agreement with the numbers in Table III. A similar good correspondence is present between the enthalpies of vaporization given by Shurtz and Hewson[53] for the liquid carbonates at 298 K and the calculated values of the present work (Table II).

The phase diagrams of the binary carbonate mixtures have already been calculated in the literature using thermodynamic mixing models in the melting equilibrium range,[1,2] and similarly good agreement between the experimental values and the calculations is obtained, as shown in Figs. 6–8 of the present work. However, in the evaluations of Liu[1] and Ding[2] a non-ideal mixing behavior was found for all binary systems, while in the present work only the liquid mixtures between cyclic and linear carbonates are described with non-ideal behavior. If, however, cyclic or linear carbonates are only mixed with each other, an ideal behavior is obtained in the present work.

Conclusions

This work presents a critical evaluation of the thermodynamic data of 5 pure organic carbonates considering the solid, liquid and gaseous phases, for which a consistent set of Gibbs energy functions is given. All five carbonates investigated are thermodynamically metastable but still sufficiently durable for experimental investigations and they are also available from commercial suppliers. Liquid mixtures of similar carbonates (cyclic with each other (EC-PC) and aliphatic with each other (DMC-EMC, DMC-DEC, EMC-DEC)) have ideal mixing behavior. Mixtures of cyclic and aliphatic carbonates have positive enthalpies of mixing. In the gas phase at atmospheric pressure, all five carbonates can be described by ideal mixing behavior.

Acknowledgments

ORCID

Peter Franke ⬡ https://orcid.org/0009-0009-3322-4004

References

1. Z.-K. Liu, *J. Electrochem. Soc.*, **150**, A359 (2003).
2. M. S. Ding, *J. Chem. Eng. Data*, **49**, 276 (2004).
3. H. L. Lukas, S. G. Fries, and B. Sundman, *Computational Thermodynamics* (Cambridge University Press, Cambridge) (2007).
4. W. Kauzmann, *Chem. Rev.*, **43**, 219 (1948).
5. A. T. Dinsdale, *Calphad*, **15**, 317 (1991).
6. J.-O. Anderson, T. Helander, L. Höglund, P. Shi, and B. Sundman, *Calphad*, **26**, 273 (2002).
7. C. J. Brown, *Acta Cryst*, **7**, 92 (1954).
8. I. A. Vasil'ev and V. M. Petrov, *Thermodynamic Properties of Oxygen-Containing Organic Compounds* (Khimiya) (1984).
9. L. Vogdanis, B. Martens, H. Uchtmann, F. Hensel, and W. Heitz, *Makromol. Chem.*, **191**, 465 (1990).
10. Y. Chernyak and J. H. Clements, *J. Chem. Eng. Data*, **49**, 1180 (2004).
11. V. Pokorný, V. Štejfa, M. Fulem, C. Červinka, and K. Růžička, *J. Chem. Eng. Data*, **62**, 4174 (2017).
12. P. Finster, J. Jung, M. Rohde, H. J. Seifert, and C. Ziebert, *Chem. Thermodyn. Therm. Anal.*, **18**, 100170 (2025).
13. C. S. Hong, R. Wakslak, H. Finston, and V. Fried, *J. Chem. Eng. Data*, **27**, 146 (1982).
14. S. P. Verevkin, A. V. Toktonov, Y. Chernyak, B. Schäffner, and A. Börner, *Fluid Phase Equilib.*, **268**, 1 (2008).
15. P. T. Thompson, R. E. Taylor, and R. H. Wood, *J. Chem. Thermodyn.*, **7**, 547 (1975).
16. J. K. Choi and M. J. Joncich, *J. Chem. Eng. Data*, **16**, 87 (1971).
17. S. P. Verevkin, V. N. Emel'yanenko, A. V. Toktonov, Y. Chernyak, B. Schäffner, and A. Börner, *J. Chem. Thermodyn.*, **40**, 1428 (2008).
18. T. F. Vasil'eva, E. N. Zhil'tsova, and A. A. Vvedenskii, *Russ. J. Phys. Chem.*, **46**, 316 (1972).
19. W. L. Calhoun, *J. Chem. Eng. Data*, **28**, 146 (1983).
20. H. Fujimori and M. Oguni, *J. Chem. Thermodyn.*, **26**, 367 (1994).
21. C. A. Angell, L. Boehm, M. Oguni, and D. L. Smith, *J. Mol. Liquids*, **56**, 275 (1993).
22. F. Comelli, R. Francesconi, A. Bigi, and K. Rubini, *J. Chem. Eng. Data*, **51**, 665 (2006).
23. V. M. Petrov and L. I. Sandler, *Zh. Fiz. Khim.*, **49**, 2797 (1975).
24. K. Nasirzadeh, R. Neueder, and W. Kunz, *J. Chem. Eng. Data*, **50**, 26 (2005).
25. Y. R. Dougassa, J. Jacquemin, L. El Ouatani, C. Tessier, and M. Anouti, *J. Chem. Thermodyn.*, **79**, 49 (2014).
26. G. M. Wilson, D. M. VonNiederhausern, and N. F. Giles, *J. Chem. Eng. Data*, **47**, 761 (2002).
27. P. S. Whitfield, *Powder Diffract*, **38**, 100 (2023).
28. V. Pokorný, V. Štejfa, M. Fulem, C. Červinka, and K. Růžička, *J. Chem. Eng. Data*, **62**, 3206 (2017).
29. J. M. Pardo, D. González-Salgado, C. A. Tovar, C. A. Cerdeiriña, and E. Romaní, *Can. J. Chem.*, **80**, 370 (2002).
30. S. Xue, K. Hou, Y. Shi, Z. Zhang, L. Fang, X. Liu, and M. He, *J. Therm. Anal. Calorim.*, **147**, 10707 (2022).
31. Y. Zhou and J. Wu, *J. Phys. Chem. Ref. Data*, **40**, 043106 (2011).
32. W. V. Steele, R. D. Chirico, S. E. Knipmeyer, and A. Nguyen, *J. Chem. Eng. Data*, **42**, 1008 (1997).
33. A. Rodríguez, J. Canosa, A. Domínguez, and J. Tojo, *Fluid Phase Equilib*, **198**, 95 (2002).
34. Y. Shi, H. Liu, K. Wang, W. Xiao, and Y. Hu, "Hu." *Fluid Phase Equilib*, **234**, 1 (2005).
35. S. A. Kozlova, V. N. Emel'yanenko, M. Georgieva, S. P. Verevkin, Y. Chernyak, B. Schäffner, and A. Börner, *J. Chem. Thermodyn.*, **40**, 1136 (2008).
36. F. Stehmann, P. Prziwara, C. Bradtmöller, M. Schoenitz, and S. Scholl, *Chem. Ing. Tech.*, **88**, 327 (2016).
37. W. V. Steele, R. D. Chirico, S. E. Knipmeyer, A. Nguyen, and N. K. Smith, *J. Chem. Eng. Data*, **42**, 1037 (1997).
38. A. A. Yakovenko, J. H. Gallegos, M. Antipin, A. Masunov, and T. V. Timofeeva, *Cryst. Growth Des.*, **11**, 3964 (2011).
39. J. M. Pardo, C. A. Tovar, C. A. Cerdeiriña, E. Carballo, and L. Romaní, *Fluid Phase Equilib.*, **179**, 151 (2001).
40. L. Becker and J. Gmehling, *J. Chem. Eng. Data*, **46**, 1638 (2001).
41. F. Comelli, A. Bigi, D. Vitalini, and K. Rubini, *J. Chem. Eng. Data*, **55**, 205 (2010).
42. K. Hou, Z. Zhang, S. Xue, X. Liu, and M. He, *J. Chem. Eng. Data*, **67**, 661 (2022).
43. A. Rodríguez, J. Canosa, A. Domínguez, and J. Tojo, *J. Chem. Eng. Data*, **47**, 1098 (2002).
44. Y. Xing, W. Fang, D. Li, Y. Guo, and R. Lin, *J. Chem. Eng. Data*, **54**, 1865 (2009).
45. B. Marrufo, S. Loras, and E. Lladosa, *J. Chem. Eng. Data*, **56**, 4790 (2011).
46. M. Månsson, *J. Chem. Thermodyn.*, **4**, 865 (1972).
47. X. Zhang, J. Zuo, and C. Jian, *J. Chem. Eng. Data*, **55**, 4896 (2010).
48. M. S. Ding, *J. Electrochem. Soc.*, **150**, A455 (2003).
49. C.-C. Hu, P.-H. Chiu, S.-J. Wang, and S.-H. Cheng, *J. Chem. Eng. Data*, **60**, 1487 (2015).
50. H.-P. Luo, J.-H. Zhou, W.-D. Xiao, and K.-H. Zhu, *J. Chem. Eng. Data*, **46**, 842 (2001).
51. Y.-J. Fang and J.-M. Qian, *J. Chem. Eng. Data*, **50**, 340 (2005).
52. R. Nagl, Z. Fan, C. Nobis, C. Kiefer, A. Fischer, T. Zhang, T. Zeiner, and M. Fischlschweiger, *J. Mol. Liquids*, **386**, 122449 (2023).
53. R. C. Shurtz and J. C. Hewson, *J. Electrochem. Soc.*, **167**, 090543 (2020).
54. R. C. Shurtz and J. C. Hewson, *J. Electrochem. Soc.*, **172**, 079001 (2025).